Published in final edited form as:
Cell Rep. 2013 November 27; 5(4): 997–1009. doi:10.1016/j.celrep.2013.10.028.

Link between Primate Lentiviral Coreceptor Usage and Nef Function

Jan Schmökel[1,7], **Hui Li**[2,7], **Asma Shabir**[1], **Hangxing Yu**[1], **Matthias Geyer**[3], **Guido Silvestri**[4], **Donald L. Sodora**[5], **Beatrice H. Hahn**[2,6], and **Frank Kirchhoff**[1,*]

[1]Institute of Molecular Virology, University of Ulm, 89069 Ulm, Germany

[2]Department of Medicine, University of Pennsylvania, Philadelphia, PA 19104, USA

[3]Center of Advanced European Studies and Research (CAESAR), Physical Biochemistry Group, 53175 Bonn, Germany

[4]Yerkes Regional Primate Research Center, Emory University, Atlanta, GA 30322, USA

[5]Seattle Biomedical Research Institute, Seattle, WA 98109, USA

[6]Department of Microbiology, University of Pennsylvania, Philadelphia, PA 19104, USA

Summary

Simian immunodeficiency virus (SIVsmm) infection of sooty mangabeys (*Cercocebus atys*) is characterized by stable $CD4^+$ T cell counts despite high plasma levels of CCR5-tropic viruses. However, in rare instances, SIVsmm acquires CXCR4 coreceptor tropism and causes severe $CD4^+$ T cell depletion, albeit without clinical signs of immunodeficiency. Here, we show that CXCR4-tropic SIVsmm strains lost their ability to downmodulate TCR-CD3 by evolving unusual Nef mutations that initially reduced (I132V) and subsequently disrupted (I123L and L146F) interaction with the CD3 ζ chain. This coevolution of Env and Nef function suggests that CD3 downmodulation is advantageous for viral replication in activated $CCR5^+$ memory T cells, but not in resting naive $CXCR4^+$ T cells that have not yet undergone TCR-CD3-mediated stimulation. This may explain why HIV-1, which generally lacks the CD3 downmodulation function, commonly switches to CXCR4 usage, whereas this is extremely rare for SIV strains that have retained this Nef activity.

*Correspondence: frank.kirchhoff@uni-ulm.de.
[7]These authors contributed equally to this work

Accession Numbers: The GenBank accession numbers for the SIVsmm *env-nef* SGA sequences reported in this paper are KF477983–KF478193.

Supplemental Information:Supplemental Information includes Supplemental Experimental Procedures, six figures, and one table and can be found with this article online at http://dx.doi.org/10.1016/j.celrep.2013.10.028.

Introduction

The great majority of sooty mangabeys (SMs) that are naturally infected with simian immunodeficiency virus (SIVsmm) maintain stable $CD4^+$ T cell counts despite high levels of viral replication (reviewed in Mir et al., 2011; Chahroudi et al., 2012). In very rare instances, however, SIVsmm infection can cause severe $CD4^+$ T cell loss, albeit in the absence of clinical disease (Milush et al., 2007; Sumpter et al., 2007). In-depth analysis of two animals with almost complete loss of $CD4^+$ T cells revealed the emergence of SIVsmm variants that switched from CCR5 (R5) to CXCR4 (X4) coreceptor usage (Milush et al., 2007, 2011). In HIV-1-infected humans, such an R5-to-X4 coreceptor switch is observed in about 50% of late-stage patients and associated with rapid $CD4^+$ T cell depletion and accelerated disease progression (Connor et al., 1997; Xiao et al., 1998). In $CD4^{low}$ sooty mangabeys, $CD4^+$ T cells are also lost, but there is no generalized chronic immune activation and no disease. These unusual $CD4^{low}$ SIVsmm infections are thus a useful model to study the interplay between viral X4 tropism, $CD4^+$ T cell loss, and generalized immune activation.

In the present study, we examined the genetic and functional evolution of *env* and *nef* genes in two experimentally SIV-infected SMs with severe $CD4^+$ T cell depletion and three additional SMs that were inoculated with plasma from one of these $CD4^{low}$ animals. We hypothesized that Env and Nef function might be linked, because coreceptor tropism determines the subsets of $CD4^+$ T cells that become infected and the accessory Nef manipulates them in multiple ways to promote efficient viral replication (reviewed in Kirchhoff et al., 2008). In particular, we hypothesized that SIVsmm Nef, which unlike HIV-1 Nef is able to suppress T cell activation and apoptosis through TCR-CD3 downmodulation (Schindler et al., 2006, 2008; Arhel et al., 2009), may contribute to the lack of immune activation and the absence of disease progression in these $CD4^{low}$ animals. Surprisingly, this was not the case. Instead, we found that many *nef* alleles of X4 SIVsmm strains were unable to downmodulate TCR-CD3 and to suppress T cell activation, while maintaining all other functions and even gaining activity in downmodulating CXCR4. Thus, the lack of the TCR-CD3 downregulation function, which is a hallmark of HIV-1 (Schindler et al., 2006, 2008; Schmökel et al., 2009), was not associated with increased immune activation in $CD4^{low}$ mangabeys. Instead, this adaptation may have been required for SIVsmm replication in naive $CXCR4^+$ T cells that usually show a resting phenotype and (unlike memory $CCR5^+$ T cells) have not undergone TCR-CD3 stimulation prior to virus infection. Thus, the loss of the CD3 modulation function of Nef may promote CXCR4 tropism and associated increased pathogenesis of HIV-1.

Results

Sequence Evolution of *env* and *nef* in SIVsmm-Infected SMs with Severe $CD4^+$ T Cell Loss

To study the genetic and functional evolution of Env and Nef in two $CD4^{low}$ sooty mangabeys (SM1 and SM2), we amplified a 3.3 kb SIVsmm *env-nef*-LTR fragment (Figure 1A) by singlegenome amplification (SGA) from 17 plasma samples obtained prior to, during, and after CD4 depletion (Figure 1B). In addition, we amplified the same fragment from nine plasma samples obtained at 2, 32, and 154 weeks postinfection (wpi) from three

sooty mangabeys (SM7, SM8, and SM9) that were inoculated intravenously with 1.5 ml of plasma from one of the $CD4^{low}$ mangabey (SM2) at 304 wpi and also exhibited rapid $CD4^+$ T cell loss (Milush et al., 2007). SGA was employed to eliminate PCR-induced artifacts and to allow assessment of linkages between Env and Nef function. In all five animals, severe $CD4^+$ T cell loss was associated with a reduction in viral RNA loads by at least two orders of magnitude (Figure 1C).

A total of 211 *env-nef*-LTR sequences were analyzed from the five SMs. Animals SM1 and SM2 were infected in October 2001 with plasma from a chronically infected sooty mangabey (FQi), which had acquired its infection in the wild (Milush et al., 2007). Sequences obtained early after infection (12 wpi) from these SMs were closely related (Figure 2, bottom) but subsequently diversified, forming animal and time-point-specific clusters (Figure S1). The 31 sequences obtained from SM2 at 304 wpi (the time point of plasma sampling for i.v. injection of SM7, SM8, and SM9) formed two lineages, referred to as “A” and “B” herein after (Figure 2, upper). Notably, all 30 sequences from SM7, SM8, and SM9 at 2 wpi were closely related to one another and interspersed with the cluster A SM2-304 sequences. In contrast, sequences derived from SM7 and SM8 at 32 or 154 wpi were more closely related to cluster B SM2-304 sequences (Figure 2). Thus, following passage of SIVsmm from SM2 to three additional animals, different members of the viral quasispecies predominated during early (cluster A) and chronic (cluster B) infection.

$CD4^+$ T Cell Loss Correlates with Increased CXCR4 Coreceptor Usage

Previous studies showed that concomitant with the $CD4^+$ T cell depletion in SM1 and SM2 viral variants emerged that exhibited an expanded coreceptor tropism, using CCR5, CXCR4, and CCR8 for entry (Milush et al., 2007). However, coreceptor usage was examined only for three time points and only in a highly sensitive cell-cell fusion assay. We thus examined the coreceptor tropism of viruses infecting SM1 and SM2 in greater detail. A total of 30 *env* alleles from eight different time points (indicated in Figures 1 and 2) were selected for functional analyses. To generate virions containing these SIVsmm Envs, we cotransfected 293T cells with vectors expressing the respective Env proteins and an *env*-defective HIV-1 luciferase reporter construct. Infection of TZM-bl cells, which express CD4 as well as R5 and X4, in the presence of X4- and R5-specific entry inhibitors (AMD3100 and SCH-D, respectively) confirmed that at 12 wpi viruses from both SM1 and SM2 used mainly R5 (Figure 3A). In contrast, Envs obtained after the loss of $CD4^+$ T cells (i.e., at 107, 304, and 340 wpi) preferentially used X4. Interestingly, Envs obtained during $CD4^+$ T cell decline (i.e., at 47 and 51 wpi) were blocked only poorly by both R5 and X4 inhibitors, suggesting alternative coreceptor usage (Figure 3A; data not shown).

To determine which alternative coreceptors were utilized, we exposed GHOST cells stably expressing CD4 and different G protein-coupled receptors to HIV-1 luciferase reporter constructs pseudotyped with the SIVsmm Env proteins of interest. We found that at 12 wpi both SM1 and SM2 Envs used predominantly R5 and GPR15 (BOB) and to a lesser extent CXCR6 (STRL33, Bonzo) for viral entry (Figures 3B and 3C). At subsequent time points, SIVsmm SM1 evolved to utilize mainly X4 (≥107 wpi; Figures 3B and 3D), whereas SIVsmm SM2 broadened its coreceptor usage to efficiently utilize X4 as well as other

coreceptors (Figures 3B, 3D, and 3E). Notably, this expanded coreceptor tropism was maintained after passage of virus from SM2 to SM7, SM8, and SM9 (Figures 3B and 3F), although Envs from these newly infected SMs mainly used CXCR4 at 154 wpi (data not shown). The coreceptor switch/expansion phase in both SM1 and SM2 (47–79 wpi in SM1 and 47 to 107 wpi in SM2) coincided with the acquisition of several amino acid changes (Figure S2), including changes in the V3 loop region of Env. However, amino acid substitutions that increased its net charge (from +4 to +7) emerged only later during infection and were associated with increased efficacy of X4-mediated viral entry (Figure 3; Table S1). The transitional Envs were generally less infectious than Envs obtained early or later during infection (Figure 3A; data not shown). Thus, the coreceptor switch from R5 to X4 in both SM1 and SM2 required complex changes in Env that were associated with reduced infectivity compared to the early R5- and late X4-tropic SIVsmm strains.

Loss of Nef-Mediated Modulation of TCR-CD3 and Suppression of T Cell Activation

To determine whether specific features of Nef were associated with the loss of $CD4^+$ T cells, we analyzed the function of a total of 61 *nef* alleles obtained at different time points from all five animals (Figure S3). As reported previously (Schindler et al., 2006), *nef* alleles were cloned into an HIV-1 NL4-3-based IRES-eGFP proviral vector coexpressing Nef and eGFP from a bicistronic RNA. Virus stocks were generated by cotransfection of 293T cells with the proviral constructs and a vector expressing the VSV-G envelope protein to transduce peripheral blood mononuclear cells (PBMCs) with high efficacy for flow cytometric analyses. These analyses showed that Nef-mediated downmodulation of CD4 and MHC-I did not change significantly throughout the course of infection (Figures 4A and 4B). In contrast, *nef* alleles derived from SM1 and SM2 after the loss of $CD4^+$ T cells exhibited a significant decline in CD3 downmodulation activity compared to those derived early during infection (Figure 4C). Four of eight *nef* alleles derived from SM2 at 304 wpi and all three *nef* genes obtained at 340 and 365 wpi were completely inactive in downmodulating CD3. This Nef function was also significantly reduced in viruses derived from SM1 at 340 and 365 wpi, although some marginal activity was retained (Figure 4C). The efficiency of Nef-mediated modulation of CD28 was higher in SM2 than in SM1, but most SM1 *nef* alleles from later time points (107–365 wpi) exhibited only marginal activity. Interestingly, Nef-mediated downmodulation of X4 increased significantly in viruses that also utilized this coreceptor (Figure 4E). When we grouped the SIVsmm constructs based on their coreceptor tropism, we noted that in both SM1 and SM2 X4 tropism was significantly associated with a loss of Nef-mediated downmodulation of TCR-CD3 and a gain of the CXCR4 modulation activity (Figure 4F). In SM1, X4 SIVsmm strains also lost the CD28 downmodulation function of Nef. Taken together, SIVsmm strains that were present early during infection and capable of TCR-CD3 modulation utilized mainly R5 in both SM1 and SM2, whereas those emerging late during infections and lacking this Nef function used predominantly X4 for entry into target cells (Figure 4G).

The SM2 304 wpi plasma sample used for inoculation of SM7, SM8, and SM9 contained a mixture of SIVsmm *nef* variants that did (cluster A, n = 17/31) or did not (cluster B, n = 14/31) downmodulate TCR-CD3. Interestingly, all *nef* alleles obtained from these three animals during acute infection (2 wpi) were active against TCR-CD3 (Figure 4C). In

contrast, most *nef* alleles derived from SM7 at 32 and 154 lacked this *nef* function, whereas those obtained from SM8 and SM9 remained active at these later time points (Figure 4C). Other Nef functions, such as modulation of CD4, CXCR4, and MHC-I did not change significantly in the three newly infected animals during follow-up, whereas the efficiency of CD28 modulation generally decreased from 2 to 154 wpi (Figures 4A–4E). These data indicate that Nef-mediated modulation of TCR-CD3 is required early in SIVsmm infection, but in certain cases becomes dispensable, or is even selected against, when the number of $CD4^+$ target cells is low.

To determine whether the loss of Nef-mediated downmodulation of CD3 in SM1 and SM2 was associated with an increased responsiveness of infected T cells to stimulation, we measured the surface expression of CD69, a marker of early T cell activation in HIV-1-infected PHA-treated PBMC cultures. These analyses showed that infected T cells expressing Nef alleles obtained after the loss of $CD4^+$ T cells also expressed increased levels of CD69 (Figure 4H). Next, we transduced Jurkat T cells containing the luciferase reporter gene under the control of an NFAT-dependent promoter (Fortin et al., 2004) with the proviral HIV-1 eGFP/Nef constructs and examined their responsiveness to activation. SIVsmm *nef* alleles obtained from SM1 and SM2 up to 107 wpi suppressed NFAT induction. In contrast, *nef* alleles obtained from both animals after 300 wpi rendered the T cells hyperresponsive to stimulation, similar to HIV-1 Nefs (Figure 4I). In agreement with previous data (Schindler et al., 2006; Khalid et al., 2012), suppression of CD69 expression and NFAT activation correlated significantly with the efficiency of Nef-mediated downmodulation of TCR-CD3 (Figure 4J). Finally, we also examined the ability of these *nef* alleles to enhance virion infectivity and to promote virus release by counteracting SM tetherin. We found that both of these Nef functions were preserved throughout the course of $CD4^{low}$ SIVsmm infection (Figure S4). Altogether, these results show that *nef* genes from late-stage X4 SIVsmm strains allowed efficient stimulation of virally infected T cells and thus had functional properties that were more reminiscent of *nef* alleles derived from HIV-1 than from R5 SIVsmm strains.

Residues I123 and L146 Are Critical for CD3 Downmodulation by SIVsmm Nef

We next examined which amino acid changes were responsible for the selective loss of the CD3 downmodulation function. Sequence alignments showed that active and inactive Nefs from SM2 differed by amino acid changes of I123L and L146F (Figure S3). These two substitutions were preceded by a substitution of I132V in SM2, and this change was also observed in most Nef alleles derived from SM1 at later time points (≥107 wpi). Notably, a naturally occurring amino acid variation at this position (I132T) specifically disrupts the CD3 downmodulation activity of HIV-2 Nef (Khalid et al., 2012). Comparison of the functional activity of SIVsmm Nefs differing in these residues showed that Nefs containing the I123L and L146F substitutions were inactive in CD3 downmodulation, whereas those containing the I132V change showed an intermediate phenotype (Figure 5A). Notably, the I123L and L146F changes always occurred in combination with one another, but never together with the I132V substitution (Figure S3).

The temporal appearance of different *nef* substitutions suggested a timeline where Nef-mediated CD3 downmodulation was initially reduced by the I132V substitution and later disrupted entirely by the I123L and L146F substitutions. To confirm the role of the latter changes in TCR-CD3 downmodulation, we analyzed a set of mutant SIVsmm Nefs differing specifically in these two residues. Combined changes of I123L and L146F disrupted the CD3 downmodulation activity in early SIVsmm SM2 Nefs, whereas the reciprocal revertant changes restored this activity in late inactive Nefs (Figure 5B). The I123L and L146F changes in Nef also affected the responsiveness of virally infected cells to stimulation and the induction of apoptosis but had no significant effect on other Nef activities, such as modulation of CD4, CD28, CXCR4, and MHC-I or enhancement of virion infectivity (data not shown).

To further define the role of residues I123 and L146 in Nef-mediated CD3 modulation, we performed fluorescence-activated cell sorting (FACS)-based internalization assays in Jurkat T cells. Predictably (Swigut et al., 2003), a control SIVmac239 Nef was highly active (Figure 5B). The SIVsmm SM2 75w-L4 and mutant 304w-H1 L123I/F146L Nefs also accelerated internalization of TCR-CD3, whereas the 75w-L4 I123L/L146F and wild-type 304w-H1 Nefs had no significant effect (Figure 5C). To examine whether residues I123 and L146 directly affected the interaction of Nef with CD3ζ, we performed FRET and coimmunoprecipitation analyses. Our results showed that the SIVmac239 Nef as well as SIVsmm 75w-L4 and 304w-H1 L123I/F146L Nefs were effective in pulling down CD3ζ (Figure 5D) and resulted in significant FRET signals (Figure 5E). Consistent with their inability to downmodulate TCR-CD3, no interaction was detected for the 75w-L4 I123L/L146F and wild-type 304w-H1 Nefs (Figures 5D and 5E). Thus, changes in residues I123 and L146 affect the ability of SIVsmm Nef to interact with the CD3ζ chain.

Next, we examined the effect of the I123L and L146F substitutions on the ability of Nef to modulate the subcellular localization of TCR-CD3. For these experiments, we utilized a previously described fusion construct between the cytoplasmic tail of CD3 and CD8 (Khalid et al., 2012). In the absence of Nef or in the presence of the HIV-1 NL4-3 and SIVsmm SM2 75-L4 I123L/L146F or 304-H1 Nef proteins, the CD8-CD3 fusion was detected at both the plasma membrane and the perinuclear regions of the cells (Figure 5F). In contrast, CD8-CD3ζ-GFP fluorescence was detected exclusively in intracellular perinuclear compartments in the presence of the SIVmac239, SIVsmm SM2 75w-L4, and 304-H1 L123I/F146L Nefs. Thus, the microscopy analyses confirmed that the I123L and L146F changes disrupt the ability of Nef to remove TCR-CD3 from the cells surface. These substitutions were present in a total of 35 *nef* alleles (14/31 SM2 304 wpi, 7/7 SM2 340/365 wpi; 5/5 SM7 32 wpi and 9/13 SM7 154 wpi sequences) that formed a distinct phylogenetic cluster (Figure 2).

To better understand how the I123L/L146F changes affected Nef-mediated modulation of TCR-CD3, we examined the localization of these residues in the crystal structure of the SIVmac239 Nef core domain complexed with the first ITAM motif of the CD3ζ chain (Kim et al., 2010). SIVmac originated from SIVsmm and Nef is highly conserved between these viruses. We found that residues I123 and L146 are located on two central α helices, which are located within the core domain of Nef (Figure 6A). These two helices are kept in place by the two gatekeeper residues F122 and Y145 (F94 and W117 in HIV- 1 Nef), which

divide the intermediate groove into a recognition site for SH3 domains and a binding site for endocytic sorting motifs (Horenkamp et al., 2011). I123 and L146 oppose each other on these two helices at a minimal distance of 4.2 Å but are not directly surface accessible (Figures 6B and 6C). Mutation to 123L and 146F, which are similarly hydrophobic but much larger, are predicted to result in a much tighter interaction between these residues (Figure 6C). Thus, the I123L and L146F changes may shift the position of the two helices relative to each other and thus alter the size and structure of the associated binding pocket in such a way that it becomes inaccessible for the CD3ζ chain but still accommodates the cytoplasmic domain of CD4, which binds the same hydrophobic crevice (Grzesiek et al., 1996).

Discussion

In the present study, we show that SIVsmm strains that switch from R5 to X4 coreceptor usage and cause severe $CD4^+$ T cell depletion gain activity in Nef-mediated downmodulation of X4 but lose their ability to remove TCR-CD3 from the cell surface (summarized in Figure S5). In one animal studied in detail, this loss of function was due to two amino acid substitutions of I123L and L148F in the core region of Nef that specifically disrupted its interaction with the TCR-CD3-ζ chain. Like X4-tropic HIV-1 strains–but unlike to common SIVsmm strains–the emerging X4-using SIVsmm variants were unable to prevent T cell activation. However, none of the five animals infected with these SIVsmm strains showed generalized immune activation or signs of disease (Milush et al., 2007, 2011). Thus, in sooty mangabeys chronic inflammation and AIDS pathogenesis requires more than $CD4^+$ T cell loss, CXCR4 tropism and loss of the Nef-mediated TCR-CD3 downregulation function. Unexpectedly, this animal model provides evidence that the latter represents an adaptation for efficient viral replication in $CXCR4^+$ T cells.

Env and Nef Coevolution

CCR5 is mainly expressed on activated memory $CD4^+$ T cells, particularly effector-memory $CD4^+$ T cells, whereas CXCR4 is predominantly expressed on quiescent or resting naive $CD4^+$ T cells. The viral Env glycoprotein determines which of these subsets of T cells are infected and the accessory Nef protein modulates the interaction of these cells with antigen-presenting cells (APCs) and their responsiveness to stimulation by downmodulation of CD4, CD28, CXCR4, and (in the case of HIV-2 and most SIVs) TCR-CD3 surface expression. Thus, it is not surprising that Env and Nef function are linked, although this has not previously been reported. The fact that X4 coreceptor utilization by rare SIVsmm variants also correlated with the efficiency of Nef-mediated downmodulation of this chemokine receptor further underscores this linkage.

Another change in Nef function that correlated with the acquisition of X4 tropism by SIVsmm was a loss of the CD3 downmodulation activity (Figure 4C). We have previously shown that this Nef function is highly conserved in HIV-2 and most lineages of SIV, but absent in HIV-1 and its *vpu* containing SIV precursors (Schindler et al., 2006, 2008; Schmökel et al., 2009; Khalid et al., 2012). CXCR4 is mainly present on naive T cells that have not yet encountered their cognate antigen and usually exhibit a quiescent or resting

phenotype that is not conducive to efficient viral replication. It is thus possible that SIVsmm tropism for $X4^+$ T cells may select for *nef* alleles that lack the CD3 modulation function because TCR-CD3 stimulation of this largely resting T cell subset by APCs may be required for effective viral replication (schematically outlined in Figure S6). In contrast, activated $CCR5^+$ memory $CD4^+$ T cells likely allow effective viral replication without further stimulation. Notably, in one animal (SM2) X4-tropic SIVsmm did not lose the TCR-CD3 downmodulation function entirely but may have compensated by also losing the CD28 downmodulation function (Figure 4F). The TCR-CD3 complex and the CD28 costimulatory factor cooperate in T cell activation. Thus, reduction of either of these Nef functions may facilitate stimulation of virally infected $CXCR4^+$ T cells by antigen-presenting cells.

R5-to-X4 Coreceptor Switch in SIVsmm, HIV-1, and HIV-2 Infection

SIVsmm strains that utilize X4 and cause rapid $CD4^+$ T cell depletion have never been detected in naturally infected SMs. Instead, the great majority of naturally infected SMs maintain high levels of $CD4^+$ T cells. In this stable host environment, activated $R5^+$ effector-memory $CD4^+$ T cells, which are the preferential targets for virus infection (Paiardini et al., 2011), are available throughout the course of infection and SIVsmm thus remains R5-tropic and active in CD3 downmodulation (schematically shown in Figure 7A). Even in the ∼10% of SMs that eventually experience a significant loss of $CD4^+$ T cells after decades of infection, this loss occurs gradually and is not associated with viral X4 coreceptor usage (Sumpter et al., 2007; Taaffe et al., 2010). It is thus surprising that after i.v. inoculation with plasma from SM FQi, SIVsmm variants capable of utilizing X4 emerged in two out of 14 animals (Silvestri et al., 2005; Milush et al., 2007; Gordon et al., 2008; Bosinger et al., 2009). Given that all Envs obtained from SM1 and SM2 early during infection utilized R5 and GPR15 (Figure 3), it is unlikely that X4 SIVsmm variants were present in the virus inoculum. Furthermore, there was no evidence for X4 viral strains in the source animal FQi, which reached an age of 22 years and died of age-related causes. Instead, the emergence of these unusual variants may have been due to the virus dose and/or the route of infection. Like in X4-tropic HIV-1 infection, the ability of SIVsmm to infect the large pool of naive $X4^+$ T cells was associated with rapid and severe $CD4^+$ T cell depletion (Figure 1B). Nonetheless, SM1 and SM2 did not develop signs of clinical immunodeficiency throughout 13 years of follow-up. A possible explanation for this is that SMs are equipped with T cells that are capable of performing helper functions but lack the CD4 receptor and are thus resistant to SIVsmm infection (Milush et al., 2011; Sundaravaradan et al., 2013).

Whereas X4 coreceptor usage is very rare in SIVsmm infection, it is observed in about 50% of late stage HIV-1-infected individuals and associated with rapid $CD4^+$ T cell decline and accelerated progression to AIDS (Moore et al., 2004). It is currently not understood which mechanisms drive X4 coreceptor usage and why this phenomenon is more common in HIV-1 than in SIV infections. Our results provide a potential explanation for the latter. *Nef* alleles lacking the CD3 downmodulation function emerged only after the drastic loss of $CD4^+$ T cells and only in the context of X4-tropic SIVsmm variants (Figure S5). Thus, lack of CD3 modulation was clearly not a cause of impaired $CD4^+$ T cell homeostasis but may have emerged as a consequence of the coreceptor switch to X4. The specific loss of the CD3

downmodulation function during the later stages of X4 SIVsmm infection in both $CD4^{low}$ SMs suggests that lack of this Nef function may be advantageous for viral replication in $X4^+$ naive T cells that have not yet undergone TCR-CD3 stimulation. We have previously shown that modulation of CD3 by Nef disrupts TCR-CD3-mediated stimulation of virally infected $CD4^+$ T cells by APCs (Arhel et al., 2009). Thus, HIV-1 and the late stage X4 SIVsmm strains analyzed in the present study may be better equipped for replication in resting naive $CXCR4^+$ T cells because they do not prevent activation of their target cells to levels required for efficient viral gene expression. It has previously been suggested that an increased number of activated $CXCR4^+$ T cells renders HIV-1-infected patients more likely to switch their coreceptor usage from R5 to X4(Weinberger and Perelson, 2011). Our results are consistent with this and suggest that X4-tropic SIVsmm strains may evolve to support the generation of activated T cells by rendering them responsive to TCR-CD3-mediated stimulation.

HIV-2 originated from SIVsmm and both are closely related. HIV-2 also shows promiscuity of coreceptor utilization but uses CXCR4 more frequently than SIVsmm, albeit less commonly than HIV-1 (Mörner et al., 1999; Calado et al., 2010). Similarly to HIV-1 infection, the acquisition of CXCR4 coreceptor usage by HIV-2 is only observed in symptomatic AIDS patients with low numbers of $CD4^+$ T cells (Guillon et al., 1998; Calado et al., 2010). Furthermore, low $CD4^+$ T cell counts are associated with reduced efficacy of TCR-CD3 downmodulation by Nef in viremic HIV-2-infected individuals (Khalid et al., 2012). These results are in agreement with a link between CXCR4 usage and Nef-mediated downmodulation of TCR-CD3 in HIV-2 infection but further studies are required to obtain definitive proof.

Nef-Mediated Suppression of T Cell Activation Is Advantageous during Acute Infection

The virus stock used to infect animals SM7, SM8, and SM9 contained two different viral lineages (“A” and “B,” Figure 2) that exhibited the same coreceptor tropism (Figure 3E) but differed in their TCR-CD3 modulation function of Nef. Approximately half of the viral sequences (14/31) amplified from the viral inoculum contained the I123L and L146M substitutions in Nef that disrupt this function. Nonetheless, all 31 *nef* alleles derived from SM7, SM8, and SM9 during acute infection at 2 wpi lacked these changes and modulated CD3. These data strongly suggest that downmodulation of CD3 is required during the earliest stages of infection. Although X4 tropism was maintained in all three animals after viral passage, the transmitted SIVsmm strains had a broad coreceptor tropism that included R5 (Figure 3). Activated $CD4^+$ T cells are readily available during acute infection and Nef-mediated downmodulation of TCR-CD3 may thus be beneficial for initial viral spread in lymphatic tissues. The finding that SIVsmm variants lacking the CD3 downmodulation function did not emerge in all SMs after severe $CD4^+$ T cell depletion suggests that infection of resting naive $CXCR4^+$ T cells may represent a suboptimal niche for SIVsmm replication in the absence of other $CD4^+$ target T cell populations.

Two Types of Changes in the Core Domain of Nef Disrupt Downmodulation of TCR-CD3

Previous mutagenesis experiments have failed to selectively eliminate CD3 downmodulation without impairing other Nef functions. In fact, the only other mutation (I132T) known to

selectively disrupt the interaction of Nef with the CD3ζ chain was identified in a variant of HIV-2 (Khalid et al., 2012). Interestingly, a change at the same position (I132V) preceded the emergence of the I123L and L146F substitutions in SM2 and also became predominant in SM1 later during infection (Figure S3). The I132V change reduced the effect of Nef on CD3 but did not disrupt it entirely (Figure 5A). I132 is located at the bottom of a hydrophobic crevice in Nef (Kim et al., 2010), and the change to a polar threonine disrupts the hydrophobic contacts formed between Nef L75 of the YxxL ITAM motif in the ζ chain of CD3 (Khalid et al., 2012). In contrast, residues I123 and L146 do not interact directly with the ζ chain of CD3. However, they determine the relative position of the two large alpha helices that border the ζ chain recognition site. It is thus possible that the big, γ-branched head group of L123 and the large aromatic F146 reposition the hydrophobic crevice of the recognition site in such way that the ζ chain of CD3 is no longer accommodated, whereas binding to the endocytic sorting motif of CD4 as well as all other Nef functions remain intact. Thus, the virus may fine-tune Nef function and thus the responsiveness of virally infected T cells to stimulation by the acquisition of subtle changes that cooperate to alter the interaction of Nef with specific cellular targets in an indirect allosteric manner and keep all essential surface properties intact.

Conclusions

In this paper, we show that the rare acquisition of X4 tropism by SIVsmm and the concomitant severe depletion of $CD4^+$ T cells are associated with changes in Nef function, i.e., increased downmodulation of X4 and loss of the ability to remove TCR-CD3 from the cell surface to suppress T cell activation. This coevolution suggests a functional linkage between Env and Nef that has previously gone unrecognized. The lack of Nef-mediated downmodulation of CD3 may enhance viral replication fitness in naive resting $CXCR4^+$ T cells, because it allows their TCR-CD3-mediated stimulation by APCs to increase virus production. Thus, lack of CD3 downmodulation may be one reason why X4 tropism is more common in HIV-1 than in SIVsmm infection.

Experimental Procedures

Animals and Viral Loads

Animals were infected and plasma viral loads and $CD4^+$ T cell counts were determined as previously described (Milush et al., 2007). Local animal care and use committee and National Institutes of Health protocols were strictly followed in the maintenance of the animals at the Yerkes National Primate Center.

Single Genome Amplification

Single genome amplification and sequencing was performed as specified in the Supplemental Experimental Procedures.

Proviral Constructs

Proviral constructs were generated as described in the Supplemental Experimental Procedures.

Envelope Expression Constructs

Full-length *env* genes were PCR amplified from the single genome amplicons as outlined in the Supplemental Experimental Procedures.

Cell Culture

Cells were cultured as described in the Supplemental Experimental Procedures.

Virus Stocks and Transductions

Virus stocks were generated and used for transduction of various cell lines as specified in the Supplemental Experimental Procedures.

Infectivity Assays

Virus infectivity was determined using TZM-bl, P4-CCR5, and GHOST cells as outlined in the Supplemental Experimental Procedures.

Flow Cytometric Analysis

CD4, TCR-CD3, MHC-I, CD28, CXCR-4 (BD Pharmingen, Clone 12G5), and eGFP reporter expression in human PBMCs transduced with HIV-1 (NL4-3) constructs coexpressing Nef and eGFP were measured as described (Schindler et al., 2008). IL-2R, CD69 expression was measured by standard FACS staining as outlined in the Supplemental Experimental Procedures.

PBMC Activation and Apoptosis

The effect of various *nef* alleles on the responsiveness of virally infected PBMCs to stimulation and subsequent induction of apoptosis was examined as described (Schindler et al., 2006). See the Supplemental Experimental Procedures for detail.

NFAT Induction

Jurkat cells stably transfected with an NFAT-dependent reporter gene vector (Fortin et al., 2004) were either left uninfected or transduced with HIV-1 Nef/eGFP constructs expressing various *nef* alleles. Except for those cells used as controls, cultures were treated with PHA (1 μg/ml; Murex). Luciferase activity was measured and n-fold induction was determined by calculating the ratio between measured relative light units of treated samples over untreated samples as described previously (Schindler et al., 2006).

Tetherin Antagonism

The ability of SIVsmm Nef proteins to counteract SM tetherin was determined as described in the Supplemental Experimental Procedures.

Microscopic Analyses

Confocal microscopy was performed as outlined in the Supplemental Experimental Procedures.

FACS-Based FRET assay

293T cells were transfected with constructs expressing CD3-ζ and Nef fusions with YFP and CFP, respectively, and interactions were determined as described previously (Banning et al., 2010).

Nef Model Building

Mutations of I123L and L146F were inserted into the SIVmac239 Nef structure and displayed using the program PyMOL (http://www.pymol.org). Sequence polarity was calculated with the program UCSF Chimera as described (Lülf et al., 2011).

Statistical Analysis

The PRISM package version 5.0 (Abacus Concepts) was used for all calculations.

Supplementary Material

Refer to Web version on PubMed Central for supplementary material.

Acknowledgments

We thank Daniela Krnavek for excellent technical assistance and Daniel Sauter for critical reading of the manuscript. TZM-bl cells were obtained through the NIH AIDS Research and Reference Reagent Program. This work was supported in part by the NIH (P01 AI 088564, R01 AI 050529, and R01 AI 066998) and the Deutsche Forschungsgemeinschaft (Leibniz award to F.K.).

References

Arhel N, Lehmann M, Clauss K, Nienhaus GU, Piguet V, Kirchhoff F. The inability to disrupt the immunological synapse between infected human T cells and APCs distinguishes HIV-1 from most other primate lentiviruses. J Clin Invest. 2009; 119:2965–2975. [PubMed: 19759518]

Banning C, Votteler J, Hoffmann D, Koppensteiner H, Warmer M, Reimer R, Kirchhoff F, Schubert U, Hauber J, Schindler M. A flow cytometry-based FRET assay to identify and analyse protein-protein interactions in living cells. PLoS ONE. 2010; 5:e9344. [PubMed: 20179761]

Bosinger SE, Li Q, Gordon SN, Klatt NR, Duan L, Xu L, Francella N, Sidahmed A, Smith AJ, Cramer EM, et al. Global genomic analysis reveals rapid control of a robust innate response in SIV-infected sooty mangabeys. J Clin Invest. 2009; 119:3556–3572. [PubMed: 19959874]

Calado M, Matoso P, Santos-Costa Q, Espirito-Santo M, Machado J, Rosado L, Antunes F, Mansinho K, Lopes MM, Maltez F, et al. Coreceptor usage by HIV-1 and HIV-2 primary isolates: the relevance of CCR8 chemokine receptor as an alternative coreceptor. Virology. 2010; 408:174–182. [PubMed: 20947116]

Chahroudi A, Bosinger SE, Vanderford TH, Paiardini M, Silvestri G. Natural SIV hosts: showing AIDS the door. Science. 2012; 335:1188–1193. [PubMed: 22403383]

Connor RI, Sheridan KE, Ceradini D, Choe S, Landau NR. Change in coreceptor use correlates with disease progression in HIV-1– infected individuals. J Exp Med. 1997; 185:621–628. [PubMed: 9034141]

Fortin JF, Barat C, Beauséjour Y, Barbeau B, Tremblay MJ. Hyper-responsiveness to stimulation of human immunodeficiency virus-infected CD4+ T cells requires Nef and Tat virus gene products and results from higher NFAT, NF-kappaB, and AP-1 induction. J Biol Chem. 2004; 279:39520–39531. [PubMed: 15258149]

Gordon SN, Dunham RM, Engram JC, Estes J, Wang Z, Klatt NR, Paiardini M, Pandrea IV, Apetrei C, Sodora DL, et al. Short-lived infected cells support virus replication in sooty mangabeys

naturally infected with simian immunodeficiency virus: implications for AIDS pathogenesis. J Virol. 2008; 82:3725–3735. [PubMed: 18216113]

Grzesiek S, Stahl SJ, Wingfield PT, Bax A. The CD4 determinant for downregulation by HIV-1 Nef directly binds to Nef. Mapping of the Nef binding surface by NMR. Biochemistry. 1996; 35:10256–10261. [PubMed: 8756680]

Guillon C, van der Ende ME, Boers PH, Gruters RA, Schutten M, Osterhaus AD. Coreceptor usage of human immunodeficiency virus type 2 primary isolates and biological clones is broad and does not correlate with their syncytium-inducing capacities. J Virol. 1998; 72:6260–6263. [PubMed: 9621102]

Horenkamp FA, Breuer S, Schulte A, Lülf S, Weyand M, Saksela K, Geyer M. Conformation of the dileucine-based sorting motif in HIV-1 Nef revealed by intermolecular domain assembly. Traffic. 2011; 12:867–877. [PubMed: 21477083]

Khalid M, Yu H, Sauter D, Usmani SM, Schmokel J, Feldman J, Gruters RA, van der Ende ME, Geyer M, Rowland-Jones S, et al. Efficient Nef-mediated downmodulation of TCR-CD3 and CD28 is associated with high CD4+ T cell counts in viremic HIV-2 infection. J Virol. 2012; 86:4906–4920. [PubMed: 22345473]

Kim WM, Sigalov AB, Stern LJ. Pseudo-merohedral twinning and noncrystallographic symmetry in orthorhombic crystals of SIVmac239 Nef core domain bound to different-length TCRzeta fragments. Acta Crystallogr D Biol Crystallogr. 2010; 66:163–175. [PubMed: 20124696]

Kirchhoff F, Schindler M, Specht A, Arhel N, Münch J. Role of Nef in primate lentiviral immunopathogenesis. Cell Mol Life Sci. 2008; 65:2621–2636. [PubMed: 18438604]

Lülf S, Horenkamp FA, Breuer S, Geyer M. Nef surfaces: where to interfere with function. Curr HIV Res. 2011; 9:543–551. [PubMed: 22103838]

Milush JM, Reeves JD, Gordon SN, Zhou D, Muthukumar A, Kosub DA, Chacko E, Giavedoni LD, Ibegbu CC, Cole KS, et al. Virally induced CD4+ T cell depletion is not sufficient to induce AIDS in a natural host. J Immunol. 2007; 179:3047–3056. [PubMed: 17709519]

Milush JM, Mir KD, Sundaravaradan V, Gordon SN, Engram J, Cano CA, Reeves JD, Anton E, O'Neill E, Butler E, et al. Lack of clinical AIDS in SIV-infected sooty mangabeys with significant CD4+ T cell loss is associated with double-negative T cells. J Clin Invest. 2011; 121:1102–1110. [PubMed: 21317533]

Mir KD, Gasper MA, Sundaravaradan V, Sodora DL. SIV infection in natural hosts: resolution of immune activation during the acute-to-chronic transition phase. Microbes Infect. 2011; 13:14–24. [PubMed: 20951225]

Moore JP, Kitchen SG, Pugach P, Zack JA. The CCR5 and CXCR4 coreceptors–central to understanding the transmission and pathogenesis of human immunodeficiency virus type 1 infection. AIDS Res Hum Retroviruses. 2004; 20:111–126. [PubMed: 15000703]

Mörner A, Björndal A, Albert J, Kewalramani VN, Littman DR, Inoue R, Thorstensson R, Fenyö EM, Björling E. Primary human immunodeficiency virus type 2 (HIV-2) isolates, like HIV-1 isolates, frequently use CCR5 but show promiscuity in coreceptor usage. J Virol. 1999; 73:2343–2349. [PubMed: 9971817]

Paiardini M, Cervasi B, Reyes-Aviles E, Micci L, Ortiz AM, Chahroudi A, Vinton C, Gordon SN, Bosinger SE, Francella N, et al. Low levels of SIV infection in sooty mangabey central memory CD^{4+} T cells are associated with limited CCR5 expression. Nat Med. 2011; 17:830–836. [PubMed: 21706028]

Schindler M, Münch J, Kutsch O, Li H, Santiago ML, Bibollet-Ruche F, Müller-Trutwin MC, Novembre FJ, Peeters M, Courgnaud V, et al. Nef-mediated suppression of T cell activation was lost in a lentiviral lineage that gave rise to HIV-1. Cell. 2006; 125:1055–1067. [PubMed: 16777597]

Schindler M, Schmökel J, Specht A, Li H, Münch J, Khalid M, Sodora DL, Hahn BH, Silvestri G, Kirchhoff F. Inefficient Nef-mediated downmodulation of CD3 and MHC-I correlates with loss of CD4+T cells in natural SIV infection. PLoS Pathog. 2008; 4:e1000107. [PubMed: 18636106]

Schmökel J, Li H, Bailes E, Schindler M, Silvestri G, Hahn BH, Apetrei C, Kirchhoff F. Conservation of Nef function across highly diverse lineages of SIVsmm. Retrovirology. 2009; 6:36. [PubMed: 19358735]

Silvestri G, Fedanov A, Germon S, Kozyr N, Kaiser WJ, Garber DA, McClure H, Feinberg MB, Staprans SI. Divergent host responses during primary simian immunodeficiency virus SIVsm infection of natural sooty mangabey and nonnatural rhesus macaque hosts. J Virol. 2005; 79:4043–4054. [PubMed: 15767406]

Sumpter B, Dunham R, Gordon S, Engram J, Hennessy M, Kinter A, Paiardini M, Cervasi B, Klatt N, McClure H, et al. Correlates of preserved CD4(+) T cell homeostasis during natural, nonpathogenic simian immunodeficiency virus infection of sooty mangabeys: implications for AIDS pathogenesis. J Immunol. 2007; 178:1680–1691. [PubMed: 17237418]

Sundaravaradan V, Saleem R, Micci L, Gasper MA, Ortiz AM, Else J, Silvestri G, Paiardini M, Aitchison JD, Sodora DL. Multifunctional double-negative T cells in sooty mangabeys mediate T-helper functions irrespective of SIV infection. PLoS Pathog. 2013; 9:e1003441. [PubMed: 23825945]

Swigut T, Greenberg M, Skowronski J. Cooperative interactions of simian immunodeficiency virus Nef, AP-2, and CD3-zeta mediate the selective induction of T-cell receptor-CD3 endocytosis. J Virol. 2003; 77:8116–8126. [PubMed: 12829850]

Taaffe J, Chahroudi A, Engram J, Sumpter B, Meeker T, Ratcliffe S, Paiardini M, Else J, Silvestri G. A five-year longitudinal analysis of sooty mangabeys naturally infected with simian immunodeficiency virus reveals a slow but progressive decline in CD4+ T-cell count whose magnitude is not predicted by viral load or immune activation. J Virol. 2010; 84:5476–5484. [PubMed: 20335252]

Weinberger AD, Perelson AS. Persistence and emergence of X4 virus in HIV infection. Math Biosci Eng. 2011; 8:605–626. [PubMed: 21631149]

Xiao L, Rudolph DL, Owen SM, Spira TJ, Lal RB. Adaptation to promiscuous usage of CC and CXC-chemokine coreceptors in vivo correlates with HIV-1 disease progression. AIDS. 1998; 12:F137–F143. [PubMed: 9764773]

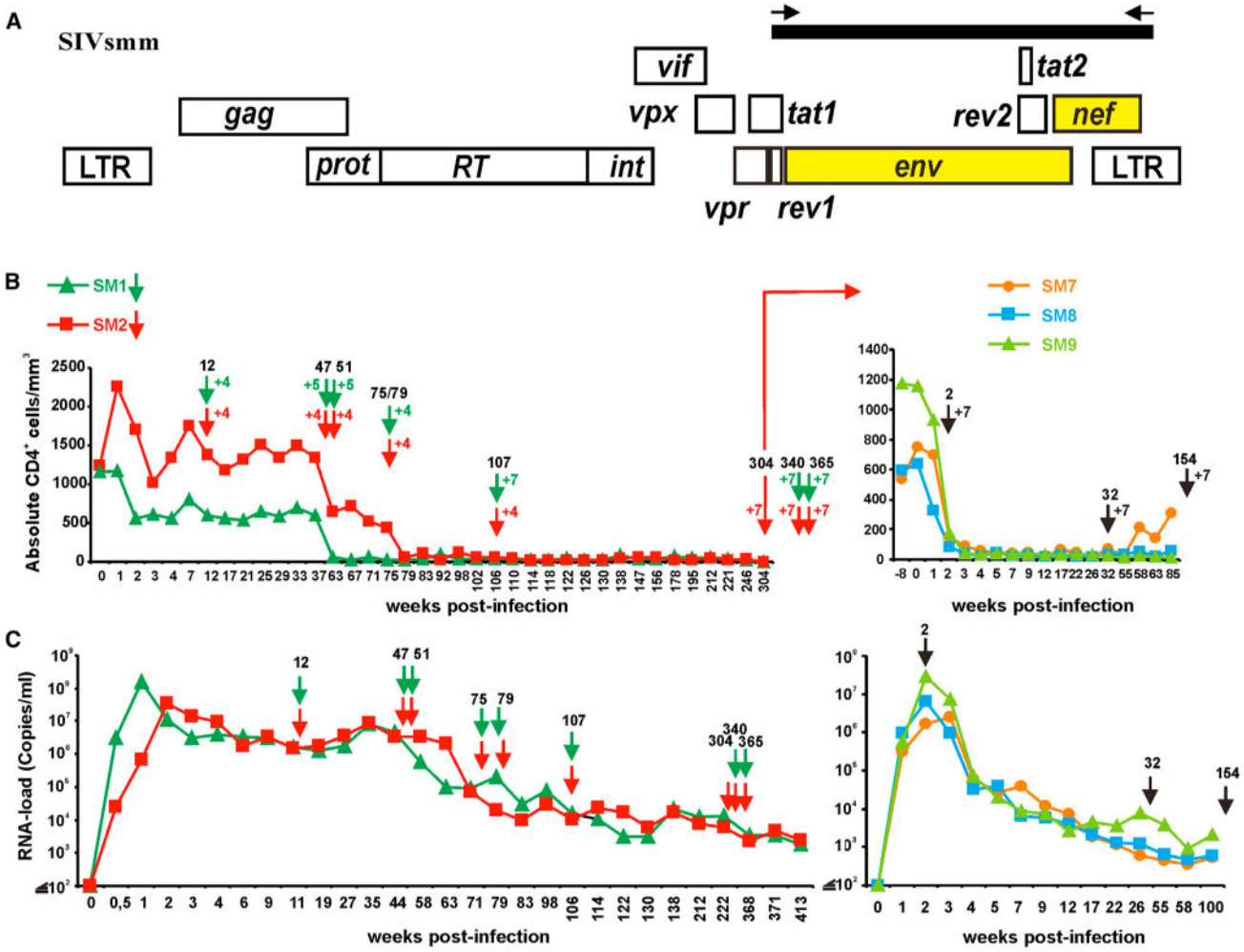

Figure 1. Longitudinal Analysis of SIVsmm env-*nef* Sequences

(A) Single-genome amplification was used to generate *env-nef* fragments from plasma samples of the SIVsmm-infected SMs indicated.

(B and C) Peripheral $CD4^+$ T cell levels (B) and viral loads (C) during the course of SIVsmm infection of the indicated animals. In SM1 and SM2, the CD4 levels declined to below 80 per µl of blood at 63 (SM1) and 79 (SM2) wpi, respectively. The loss of $CD4^+$ T cells was associated with declining plasma viral loads in all five animals. The arrows above the curves indicate the time points of plasma sampling for SGA analysis. The numbers next to the arrows indicate the predominant charge of the V3 loop amino acid sequences amplified at the corresponding time points. The time point of plasma sampling for passage of the X4/multitropic SIVsmm from SM2 to SM7, SM8, and SM9 is indicated.

See also Figure S1.

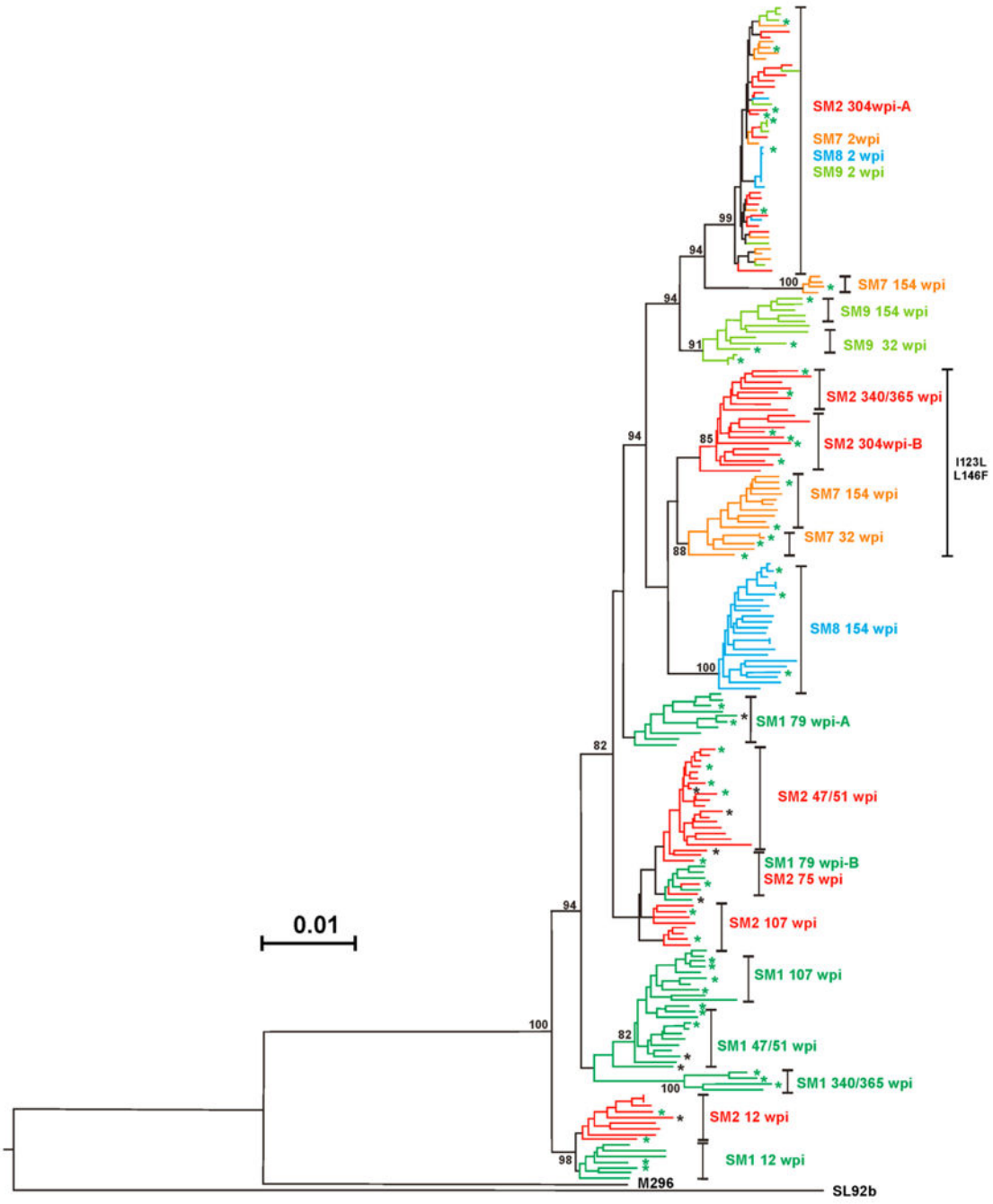

Figure 2. Evolutionary Analysis of SIVsmm *env-nef* Sequences

A phylogenetic tree was constructed using the neighbor-joining (NJ) method. The scale bar represents 0.01 substitutions per site. Sequences are color-coded based on their animal origin. Two clusters that include *nef* alleles with amino acid substitutions I123L and L146F are indicated. Stars indicate SGA sequences used to examine the function of Env and Nef (green) or Nef only (black). The length of the amplicons was about 3.7 kb. See also Table S1.

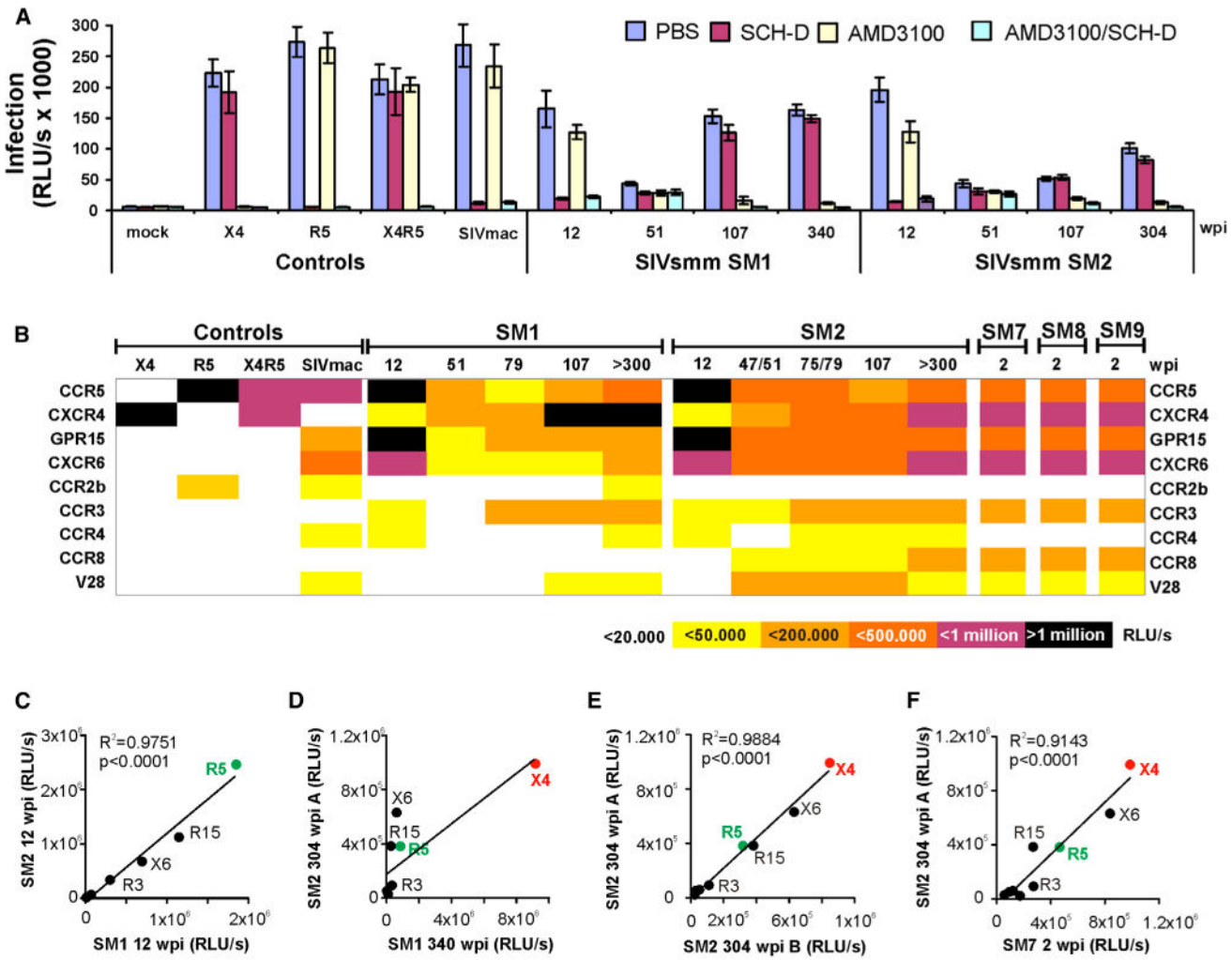

Figure 3. Longitudinal Analysis of Coreceptor Utilization in SIVsmm-Infected SMs with Severe CD4$^+$ T Cell Depletion

(A) TZM-bl cells were left untreated or treated with the CXCR4 antagonist AMD3100 (10 μM) and/or the CCR5 antagonist SCH-D (10 μM) and subsequently infected with luciferase-expressing HIV-1 virions pseudotyped with Env glycoproteins derived from SIVsmm-infected SM1 and SM2 at the indicated weeks postinfection. The Env proteins of X4- (NL4-3), R5- (BORI), and dual-tropic (WEAU) HIV-1 strains and SIVmac239 were used as controls. Virus stocks were normalized for p24 content (2 ng). Shown are average values (±SD) from two independent experiments each performed in triplicate. For each time point, results obtained for one *env* allele out of one to three analyzed are shown.

(B) GHOST cells expressing CD4 and the indicated coreceptors were infected with luciferase reporter viruses pseudotyped with various Envs as described in (A). Values were calculated from two independent experiments each performed in triplicate. Background luciferase values obtained for the parental GHOST.CD4-only cell line were deduced from those obtained with the cell lines expressing the various coreceptors.

(C–F) Correlation between the coreceptor tropism of SIVsmm Envs derived from SM1 and SM2 during the early (C) and late (D) stage of infection; (E) SM2 at 304 wpi that differed in

the CD3 modulation function of Nef (group A, 304-A1, and group B, 304-K2) and (F) the SM2 plasma sample used for virus passage and the SIV strain detected early in infection of SM7. Values represent averages of triplicate infections and were confirmed in an independent experiment. Abbreviations: R2b, CCR2b; R3, CCR3; R5, CCR5; R15, GPR15; X4, CXCR4; X6, CXCR6.

See also Figure S2.

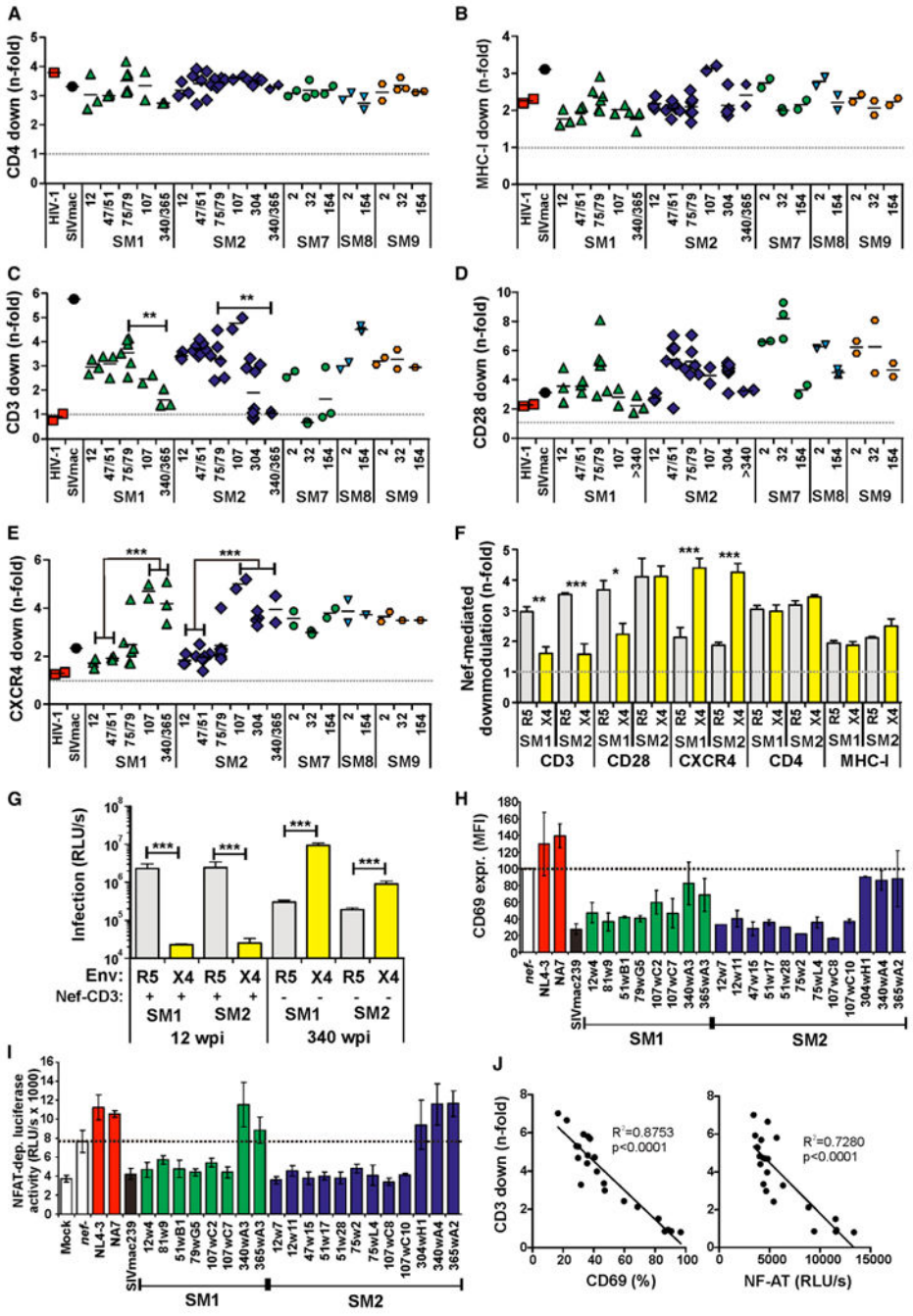

Figure 4. Selective Loss of Nef-Mediated TCR-CD3 Downmodulation and Inhibition of T Cell Activation during the Late Stages of SM Infection

(A–E) Quantitative assessment of Nef-mediated downmodulation of the indicated cellular receptors on PBMCs (CD4, CD3, CD28, and MHC-I) and Jurkat cells (CXCR4). SIVsmm *nef* genes were grouped by the time points they were derived from the SIVsmm-infected animals. Each symbol represents n-fold downmodulation of the indicated receptor molecule by one of the 60 HIV-1 NL4-3 recombinants expressing time-point representative primary

SIVsmm *nef* alleles. Similar results were obtained in an independent experiment. p values <0.05 are indicated.

(F) Nef function of SIVsmm strains differing in coreceptor tropism. Values represent the average (±SD) Nef-mediated downmodulation efficiencies of SIVsmm strains that use R5 (n = 14) or X4 (n = 8) as major entry coreceptors, respectively.

(G) Coreceptor utilization of SIVsmm strains differing in Nef function. Values represent the average (±SD) entry efficiencies of representative SIVsmm Envs obtained early or late during infection of SM1 and SM2 strains into GHOST cells expressing R5 or X4, respectively. The corresponding *nef* alleles were active (+) or inactive (−) in Nef-mediated downmodulation of TCR-CD3.

(H) Levels of CD69 expression on PBMCs transduced with HIV-1 constructs expressing Nef alleles from SIVsmm-infected SMs showing declining $CD4^+$ T cell counts at different weeks postinfection. The mean fluorescence activities (MFIs) of CD69 expression were determined at 1 days poststimulation and are shown relative to the *nef*-defective control construct.

(I) Analysis of Jurkat cells stably transfected with an NFAT-dependent reporter gene (Fortin et al., 2004) following transduction with the indicated HIV-1 Nef/eGFP constructs and subsequent stimulation with PHA. Levels of NFAT-dependent luciferase reporter activity are the average (±SD) of triple infections. Similar results were obtained in two independent experiments. Mock specifies uninfected control cells. The levels of luciferase activity in *nef*-defective virus infection are indicated by broken lines.

(J) Correlation between the efficiencies of Nef-mediated downmodulation of CD3 and CD69 cell surface expression (left) or NF-AT activity (right).

See also Figure S3.

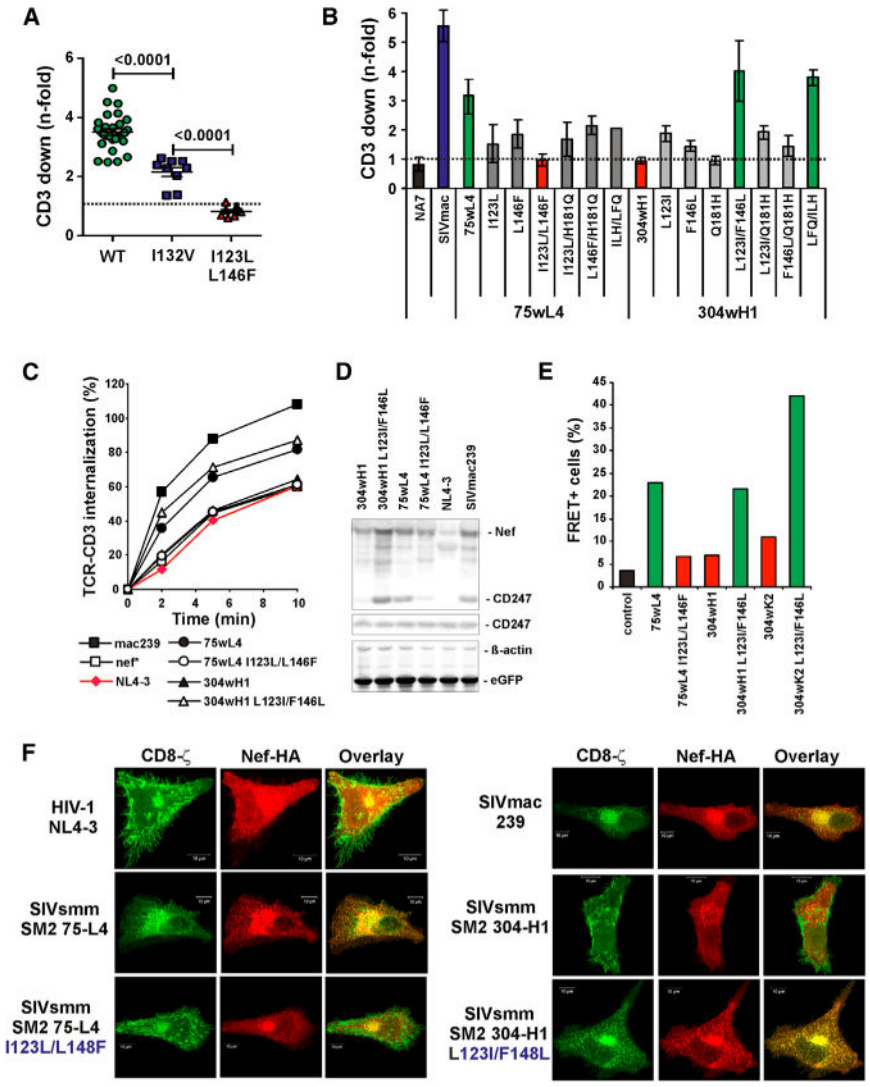

Figure 5. Amino Acid Residues I123 and L146 in SIVsmm Nef Are Critical for CD3 Downmodulation and Binding

(A) All *nef* alleles were grouped based on the presence of parental residues at positions I123, I132, and L146 (n = 28), the I132V variation (n = 9), and the I123L and L146F changes (n = 9). Each data point represents the average of three measurements.

(B) Quantitative assessment of Nef-mediated downmodulation of CD3 cell surface expression on PBMCs infected with HIV-1 Nef/eGFP constructs expressing eGFP alone (*nef*-) or together with the indicated control and primary SIVsmm FBr *nef* alleles (75wL4, 304wH1, 304wK2) and specific mutants thereof. Shown are averages ±SD derived from three independent experiments. (C) Changes in amino acids I123 and L146 impair the ability of SIVsmm Nef to accelerate endocytosis of TCR-CD3. Shown are the rates of CD3 endocytosis in the absence or presence of the indicated Nef alleles in transiently transfected Jurkat T cells determined by a fluorescence-activated cell sorting-based endocytosis assay.

(D) Coprecipitation of CD3 zeta chain by the indicated SIVsmm Nef proteins.

(E) FRET signal between the indicated Nef variants and TCR-CD3.

(F) Effect of mutations at positions 123 and 146 in the SIVsmm Nef on subcellular localization of CD8 fusions with the cytoplasmic domain of the CD3ζ chain. 293T cells were cotransfected with plasmids expressing the indicated *nef* alleles and a constructs expressing CD8 fused to the cytoplasmic domain of the CD3ζ chain. Cells were permeabilized, stained with CD8 and HA antibodies, and examined by confocal microscopy. Results are representative for at least 12 cells examined.
See also Figure S4.

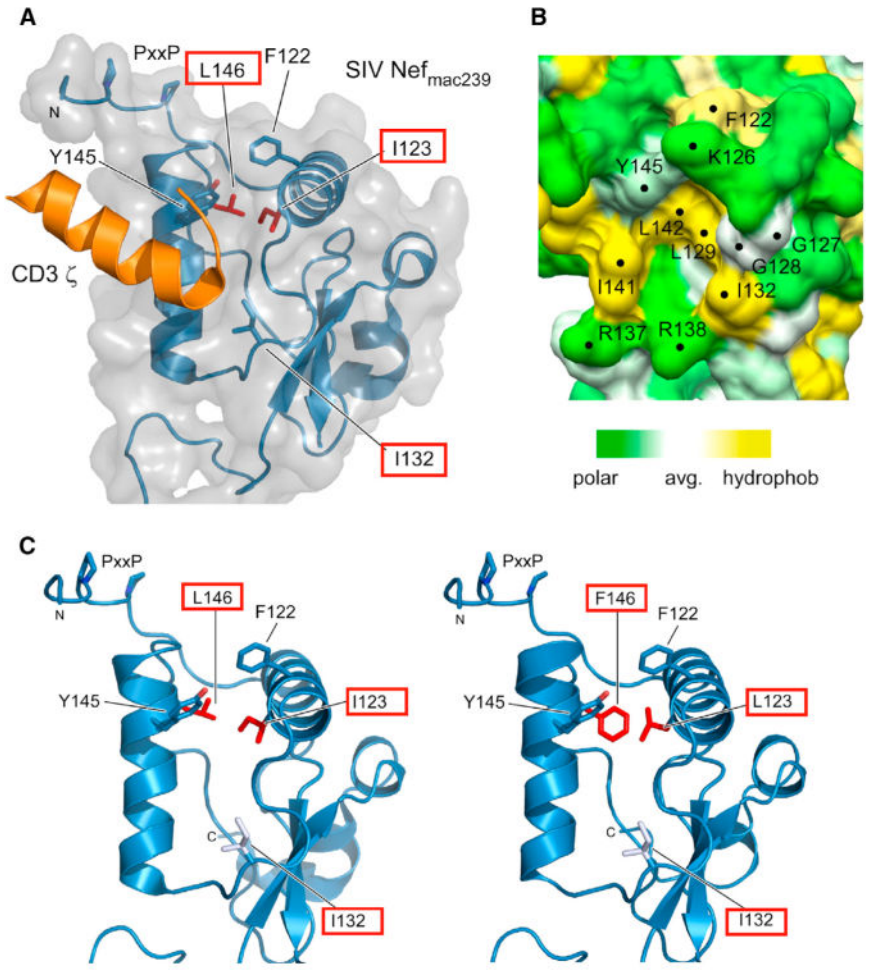

Figure 6. Localization of Amino Acids Critical for CD3 Downmodulation in the Complex between SIV Nef and CD3ζ

(A) Display of the core domain structure of SIVmac239 Nef (gray and blue) with the first ITAM motif of CD3ζ indicated in orange. Residue I132 is located at the surface of Nef and involved in CD3ζ interaction. In contrast, I123 and L146 are not accessible at the surface but located on the two central α helices that form the hydrophobic crevice accommodating the CD3ζ binding site.

(B) Close-up view of Nef residues forming the CD3ζ-Nef binding site indicating the hydrophobicity of the sorting motif binding site in SIV Nef. (C) Structural display of the I123 and L146 residues in wild-type Nef (left) and model of the two mutant sites I123L and L146F underlying the gatekeeper residues F122 and Y145 in mutant Nef (right). The spacious hydrophobic residues may perfectly fill in between the central helices and change the plasticity of the CD3 binding site (in an allosteric manner). Please note that the right only represents a structural model illustrating the localization of the I123L and L146F changes in the published Nef structure. Molecular diagrams were drawn with PyMOL (http://www.pymol.org).

See also Figure S5.

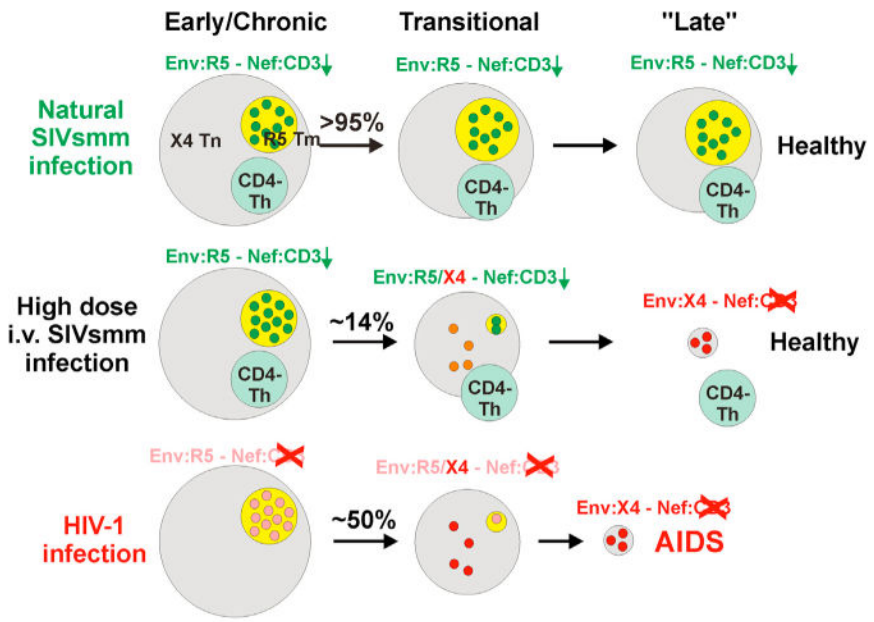

Figure 7. Characteristics of Regular and CD^{low} SIVsmm and HIV-1 Infection

Top: In the great majority of natural SIVsmm infections, the virus remains R5 tropic and capable of downmodulating TCR-CD3 to suppress T cell activation. Effective viral replication occurs mainly in activated CD4$^+$ T cells that have a short lifespan, whereas the naive and memory CD4$^+$ T cell pools decline only slightly with the increasing age of the animals. Middle: Experimental i.v. infection of SMs with relatively high doses of SIVsmm may deplete activated R5$^+$ CD4$^+$ T cells faster and thus promote the emergence of SIVsmm variants capable of infecting X4$^+$ naive T cells. Coreceptor switch to infect the large X4$^+$ T cell pool may facilitate the loss of the TCR-CD3 modulation activity of Nef because most of these cells have not yet undergone TCR-mediated stimulation. A subset of helper T cells that is resistant to SIV infection because it lacks CD4 may allow these animals to remain immunocompetent in the absence of CD4$^+$ T cells (Milush et al., 2011). Bottom: HIV-1 may be more prone to eliminate the R5$^+$ memory subset of CD4$^+$ T cells and to evolve the ability to replicate in X4$^+$ naive CD4$^+$ T cells because it generally lacks the CD3 downmodulation function of Nef. Depletion of CD4$^+$ T cells results in disease progression because humans lack compensatory CD4$^-$ helper T cells (Sundaravaradan et al., 2013).

See also Figure S6.